SIAM J. APPL. MATH.
Vol. 48, No. 6, December 1988

006

THE RIEMANN PROBLEM NEAR A HYPERBOLIC SINGULARITY II*

E. ISAACSON† AND B. TEMPLE‡

Abstract. This paper is interested in classifying the solutions of Riemann problems for the 2×2 conservation laws that have homogeneous quadratic flux functions. Such flux functions approximate an arbitrary 2×2 system in a neighborhood of an isolated point where strict hyperbolicity fails. Here the solution for the symmetric systems in Region III of the four region classification of Schaeffer and Shearer is given. The solution is based on the qualitative shape of the integral curves described by Schaeffer and Shearer and a numerical calculation of the Hugoniot loci and their shock types.

Key words. Riemann problem, nonstrictly hyperbolic conservation laws, umbilic points

AMS(MOS) subject classifications. 65M10, 76N99, 35L65, 35L67

1. Introduction. This is the second in a series of papers [5] in which we give the solution of the Riemann problem for quadratic conservation laws

$$u_t+\tfrac{1}{2}\{a_1u^2+2b_1uv+c_1v^2\}_x=0,$$
$$v_t+\tfrac{1}{2}\{a_2u^2+2b_2uv+c_2v^2\}_x=0,$$

with initial data

$$\mathbf{u}(x,0)=\begin{cases}\mathbf{u}_L\equiv(u_L,v_L), & x<0,\\ \mathbf{u}_R\equiv(u_R,v_R), & x>0,\end{cases}$$

where $\mathbf{u}\equiv(u,v)$. This is one of the steps in a program outlined in [6].

Solutions of such conservation laws approximate the solutions of a general 2×2 system of conservation laws in a neighborhood of an isolated point at which strict hyperbolicity fails.

We use the normal form

$$\begin{aligned}&u_t+\tfrac{1}{2}\{au^2+2buv+v^2\}_x=0,\\ &v_t+\tfrac{1}{2}\{bu^2+2uv\}_x=0\end{aligned}\tag{1}$$

of Schaeffer and Shearer [12].

We let $\lambda_1(\mathbf{u})\leqq\lambda_2(\mathbf{u})$ denote the eigenvalues of system (1); we note that for system (1), $\lambda_1=\lambda_2$ only when $\mathbf{u}=\mathbf{0}$, in which case $\lambda=0$.

In the first paper [5], we presented the solution of the Riemann problem for the range of parameter values

$$a>2, \qquad b=0.$$

* Received by the editors December 15, 1986; accepted for publication June 12, 1987.

† Department of Mathematics, University of Wyoming, Laramie, Wyoming 82071. The work of this author was supported in part by National Science Foundation grant DMS-831229, Department of Energy contract DE-AC02-76ER03077, University of Wyoming Division of Basic Research, Air Force Office of Scientific Research grant AFOSR-85-0117 and CNPq/Brazil grant 403039/84-MA.

‡ Department of Mathematics, University of California, Davis, California 95616 and Department of Mathematics and the Mathematics Research Center, University of Wisconsin-Madison, Madison, Wisconsin 53705. The work of this author was supported in part by FINEP/Brazil grant 4.3.82.017.9, CNPq/Brazil grant 1.01.10.011/84-ACI, National Science Foundation grant 527428INT-8415209, the U.S. Army under contract DAAG29-80-C-0041 and is based upon work supported by the National Science Foundation grants DMS-8210950, Mod. 1 and DMS-8210950, Mod. 4.

This corresponds to the symmetric systems in Region IV of [12], [5]. In the present work we give the solution of the Riemann problem for the parameter range

$$1 < a < 2, \qquad b = 0,$$

which corresponds to the symmetric systems in Region III. The solutions consist of (portions of) the 1-wave curves $\mathcal{W}_1(\mathbf{u})$ and the 2-wave curves $\mathcal{W}_2(\mathbf{u})$. These are obtained from the Hugoniot loci and integral curves by means of both numerical and analytical evidence. Our constructions indicate the following result.

THEOREM. *For each pair of states* $\mathbf{u}_L$ *and* $\mathbf{u}_R$, *there exists an intermediate state* $\mathbf{u}_M \in \mathcal{W}_1(\mathbf{u}_L)$ *such that* $\mathbf{u}_R \in \mathcal{W}_2(\mathbf{u}_M)$ *and the solution of the Riemann problem consists of the* 1*-wave from* $\mathbf{u}_L$ *to* $\mathbf{u}_M$ *followed by the* 2*-wave from* $\mathbf{u}_M$ *to* $\mathbf{u}_R$. *Moreover, the solution is unique in* x,t*-space, depends continuously on* $\mathbf{u}_L$ *and* $\mathbf{u}_R$, *and all shocks appearing in solutions are* 1*-shocks or* 2*-shocks in the sense of Lax* [9].

We refer to [5] for a detailed discussion of the problems and the notation.

We obtain the shapes and shock types of Hugoniot loci $\mathcal{H}(\mathbf{u}_L)$ by means of numerical calculation. This, together with the qualitative features of the integral curves given by [12], [2] (see Fig. 1), is the basis for our construction of the solutions. We present the solution of the Riemann problem in a series of diagrams for representative values of $\mathbf{u}_L$.

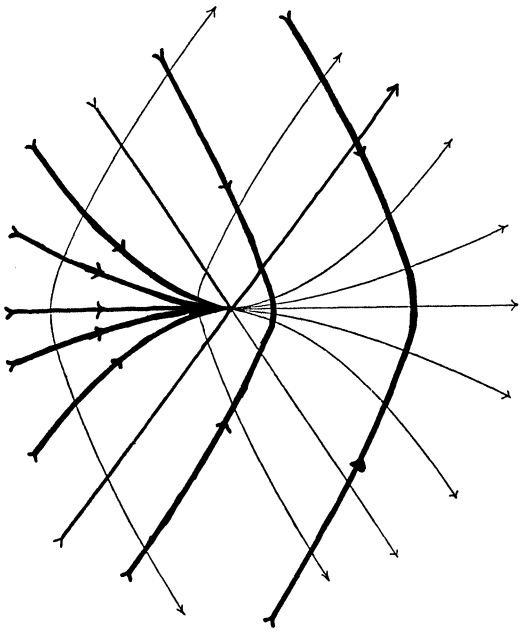

FIG. 1. *Integral curves.*

The qualitative features of the solution diagrams change precisely when $\mathbf{u}_L$ crosses $\mathcal{H}(\mathbf{0})$ or crosses a ray $\lambda_1 = 0$. In Regions I–III the Hugoniot locus $\mathcal{H}(\mathbf{0})$ consists of three straight lines (called axes), while in Region IV this locus is a single line [12]. For the symmetric systems in Regions I–III (i.e., $a < 2$, $b = 0$), one of the axes is the u-axis and the other two are given by

$$v = \pm\sqrt{2-a}\, u.$$

The rays $\lambda_1 = 0$ are given by

$$v = \begin{cases} -\sqrt{a}\, u & \text{in the lower half plane,} \\ +\sqrt{a}\, u & \text{in the upper half plane.} \end{cases}$$

We give the solution of the Riemann problem for representative values of $\mathbf{u}_L$ in the lower half plane ($v \leqq 0$) because of the symmetries in system (1) (see [5]). Since the solutions change qualitatively only at the rays $\mathscr{H}(\mathbf{0})$ and $\lambda_1 = 0$, we choose a representative value of $\mathbf{u}_L$ from each interior and bounding ray of the sectors (see Fig. 2):

$$\mathscr{A}_1 = \{\mathbf{u}\colon \theta_{12} < \theta < 0\},$$

$$\mathscr{A}_2 = \{\mathbf{u}\colon \theta_* < \theta < \theta_{12}\},$$

$$\mathscr{A}_3 = \{\mathbf{u}\colon \theta_{34} < \theta < \theta_*\},$$

$$\mathscr{A}_4 = \{\mathbf{u}\colon -\pi < \theta < \theta_{34}\},$$

where

$$\theta_{12} = \arctan(-\sqrt{2-a}),$$

$$\theta_{34} = \arctan(+\sqrt{2-a}) - \pi,$$

$$\theta_* = \arctan(-\sqrt{a}).$$

The angles correspond to the axes and the ray $\lambda_1 = 0$, respectively.

A new feature in Region III is that the Hugoniot locus $\mathscr{H}(\mathbf{u}_L)$ and the 1-wave curve $\mathscr{W}_1(\mathbf{u}_L)$ can be disconnected [5]. This makes the solutions more complicated than those found in Region IV.

In § 2 we describe the elementary waves and Hugoniot loci, and in § 3 we present the solution of the Riemann problem.

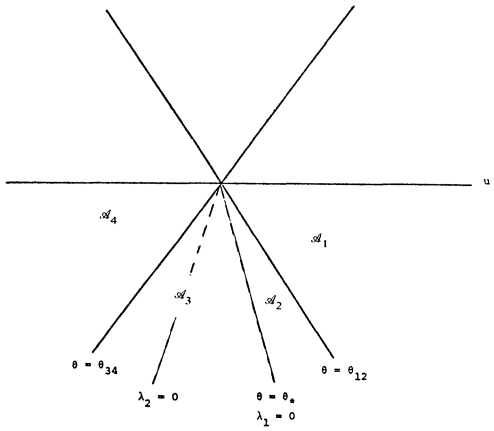

FIG. 2. *The sectors $\mathscr{A}_1$-$\mathscr{A}_4$ and their boundaries.*

2. Elementary waves. The rarefaction waves of system (1) are obtained from the integral curves of the eigenvector fields of the Jacobian $A(\mathbf{u})$. The shock waves of system (1) are obtained from the Hugoniot loci. The general solution of the Riemann problem that we construct is obtained by composing these waves. The solution consists of a 1-composite wave followed by a 2-composite wave, where a p-composite wave is a succession of shock and rarefaction waves of the p family [5]. The p-wave curve $\mathscr{W}_p(\mathbf{u}_L)$ consists of all final states in p-composite waves with initial state $\mathbf{u}_L$.

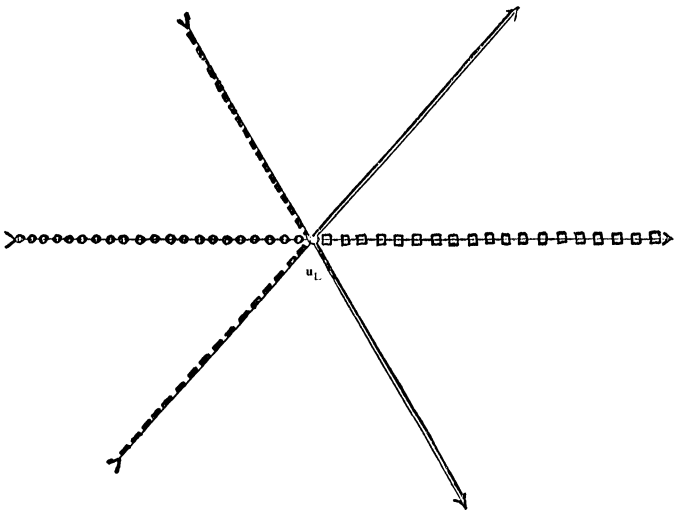

FIG. 3(a). *The Hugoniot locus* $\mathscr{H}(\mathbf{u}_L)$ *for* $\mathbf{u}_L = \mathbf{0}$.

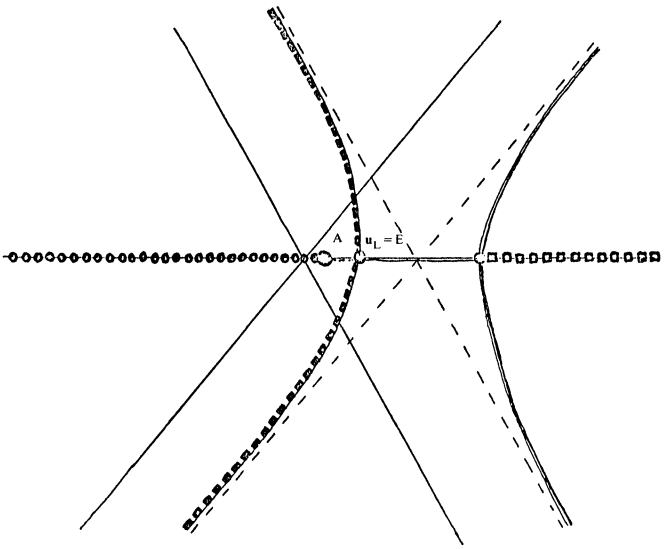

FIG. 3(b). *The Hugoniot locus* $\mathscr{H}(\mathbf{u}_L)$ *for* $\theta_L = 0$.

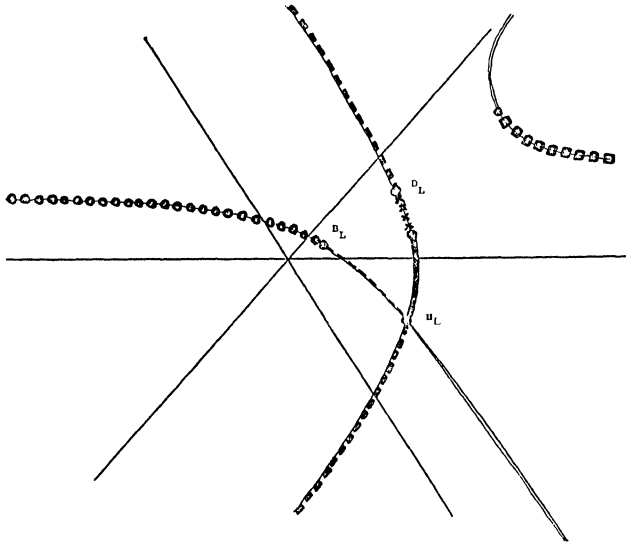

FIG. 3(c). *The Hugoniot locus* $\mathscr{H}(\mathbf{u}_L)$ *for* $\mathbf{u}_L \in \mathscr{A}_1$.

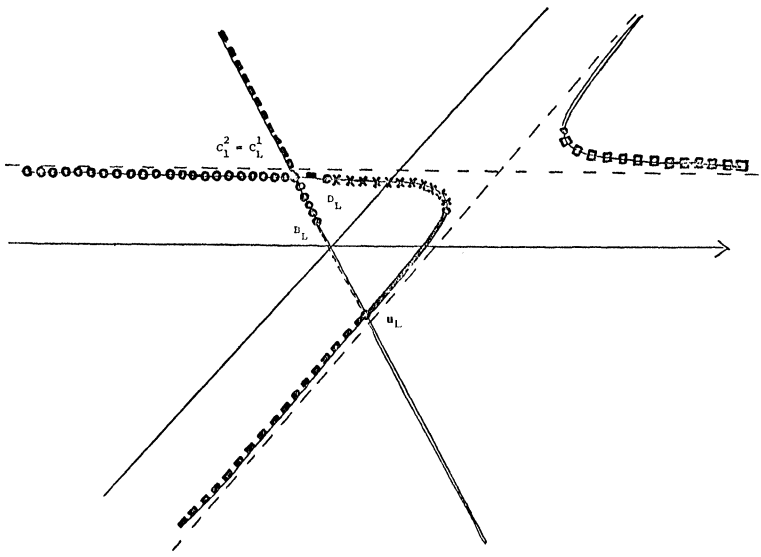

FIG. 3(d). *The Hugoniot locus* $\mathscr{H}(\mathbf{u}_L)$ *for* $\theta_L = \theta_{12}$.

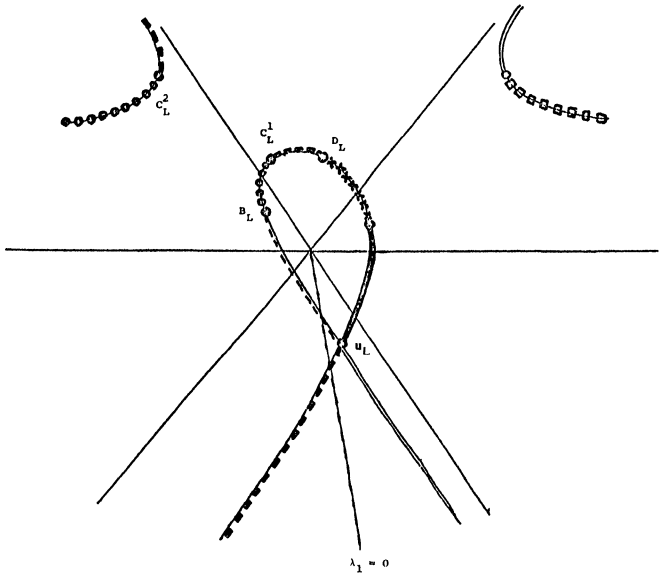

FIG. 3(e). *The Hugoniot locus* $\mathscr{H}(\mathbf{u}_L)$ *for* $\mathbf{u}_L \in \mathscr{A}_2$.

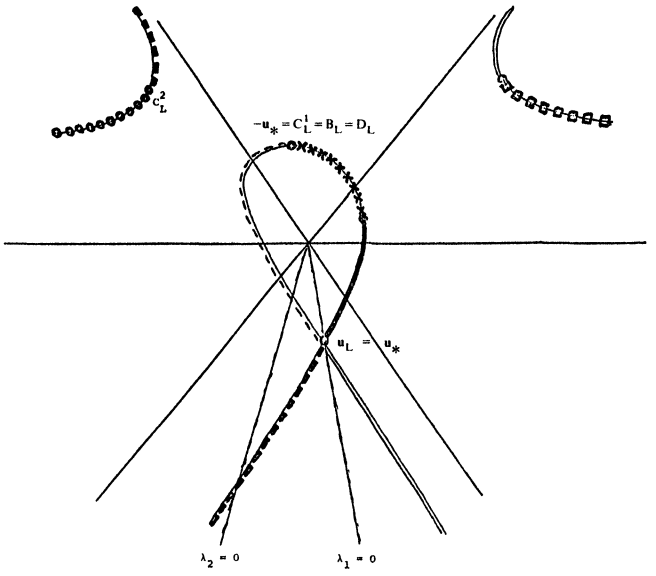

FIG. 3(f). *The Hugoniot locus* $\mathscr{H}(\mathbf{u}_L)$ *for* $\theta_L = \theta_*$.

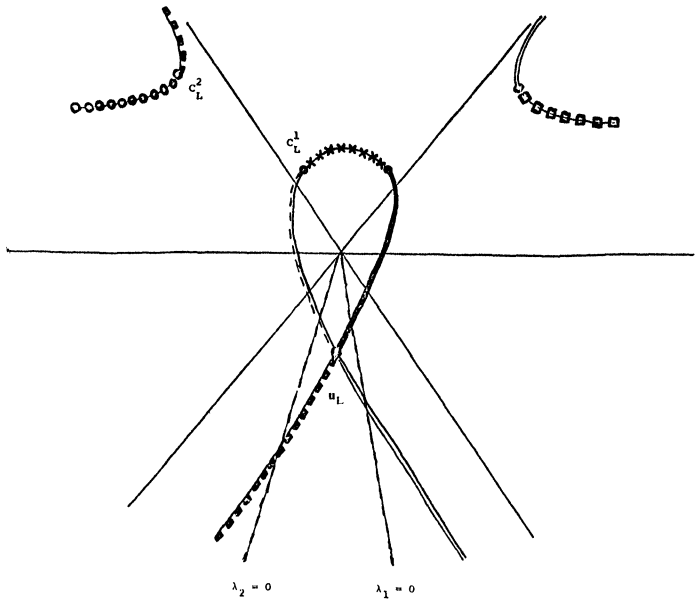

FIG. 3(g). *The Hugoniot locus* $\mathscr{H}(\mathbf{u}_L)$ *for* $\mathbf{u}_L \in \mathscr{A}_3$.

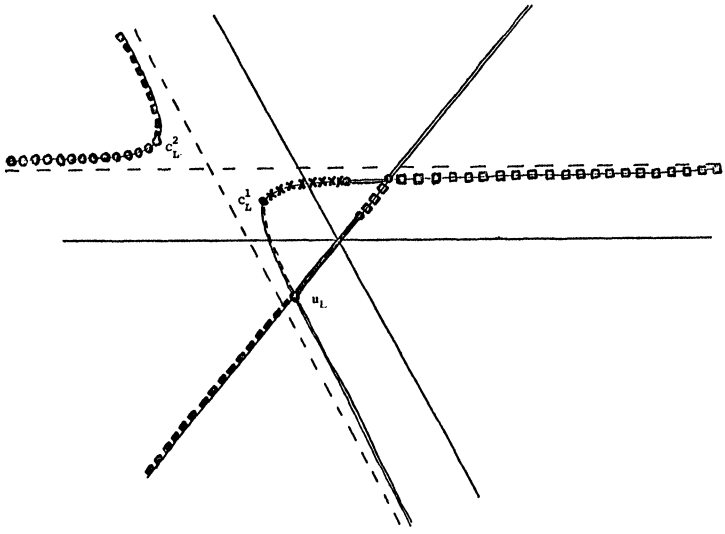

FIG. 3(h). *The Hugoniot locus* $\mathscr{H}(\mathbf{u}_L)$ *for* $\theta_L = \theta_{34}$.

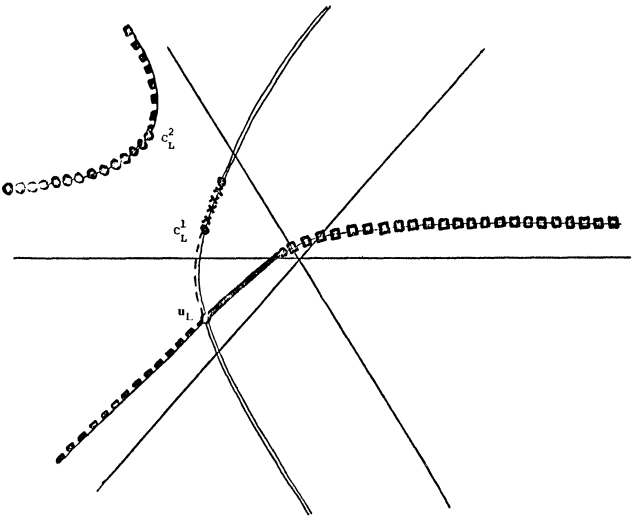

FIG. 3(i). *The Hugoniot locus* $\mathscr{H}(\mathbf{u}_L)$ *for* $\mathbf{u}_L \in \mathscr{A}_4$.

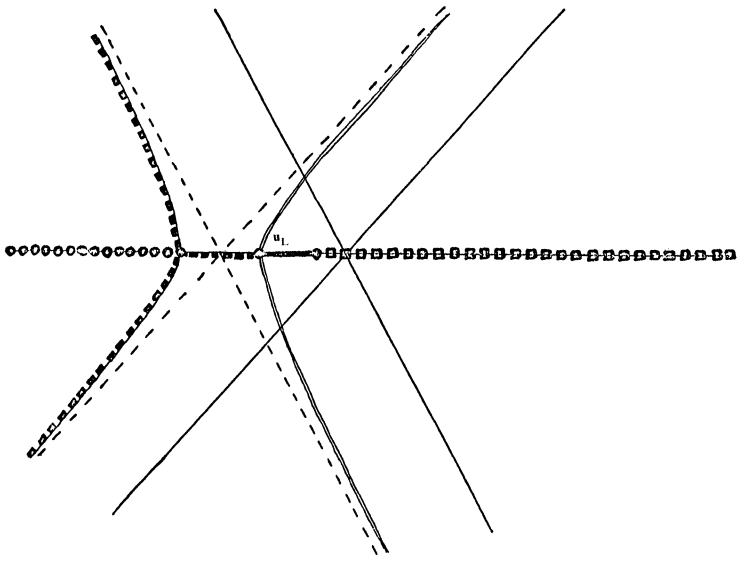

FIG. 3(j). *The Hugoniot locus* $\mathscr{H}(\mathbf{u}_L)$ *for* $\theta_L = -\pi$.

The qualitative shapes of the integral curves for the symmetric systems (1) in Region III are depicted in Fig. 1 (see [12], [2]).

2.1. Hugoniot loci. The structure of the Hugoniot loci is depicted in Figs. 3(a)-(j) for representative values of $\mathbf{u}_L$. These figures indicate the general topological structure of the loci as well as the location of shock types. As $\mathbf{u}_L$ varies, these features change qualitatively only at the boundaries of the sectors $\mathscr{A}_1$-$\mathscr{A}_4$ (and at $\lambda_2 = 0$). The topological structure of the Hugoniot locus changes at the axes, while at the lines $\lambda = 0$ the topological structure remains fixed but the location of shock types changes. (We do not include $\lambda_2 = 0$ as a boundary since the change in shock types at $\lambda_2 = 0$ does not affect the Riemann problem solutions. Specifically, the wave curves, and hence solutions, do not change qualitatively at $\lambda_2 = 0$.)

Note that the Hugoniot loci of states in quadrant IV of the u,v-plane determine all Hugoniot loci, because the reflection of a Hugoniot locus about either the u- or v-axis is again a Hugoniot locus [5]. For clarity, we include the Hugoniot loci for sector $\mathscr{A}_4$ and its boundary rays $\theta = -\pi$, $\theta = \theta_{34}$ because these are relevant to the solution of the Riemann problem.

2.2. Special points. In Figs. 4(b)-(g), E is a fixed point on the positive u-axis, and $\mathbf{u}_L$ is taken on the integral curve through E. The point A is the limit of the intersection of $\mathscr{H}(\mathbf{u})$ with the positive u-axis as $\mathbf{u}$ tends to E through states with $v \neq 0$.

In Figs. 3(c)-(f) and 4(c)-(f), the points B_L and D_L are the points on $\mathscr{H}(\mathbf{u}_L)$ at which

$$\sigma(\mathbf{u}_L, B_L) = \lambda_1(\mathbf{u}_L) = \sigma(\mathbf{u}_L, D_L).$$

Necessarily, $\{\mathbf{u}_L, D_L, B_L\}$ is a triple shock [5].

In Figs. 3(d)-(i) and 4(d)-(i), the points C_L^1 and C_L^2 are the points at which $\mathscr{H}(\mathbf{u}_L)$ is tangent to a 2-integral curve.

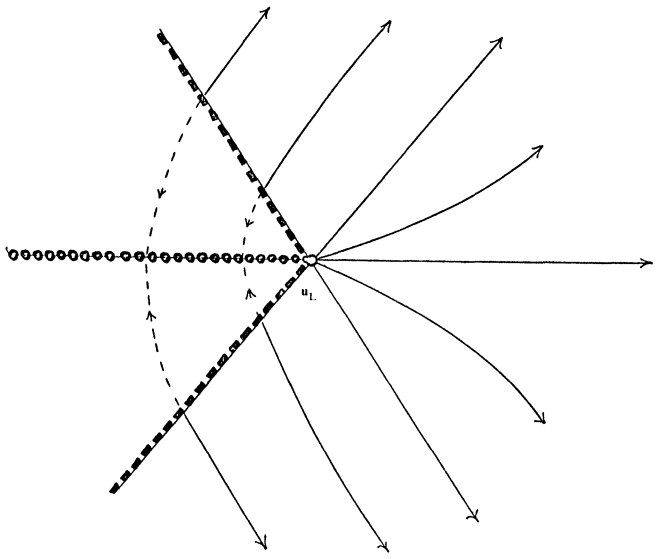

FIG. 4(a). *Solution diagram for* $\mathbf{u}_L = \mathbf{0}$.

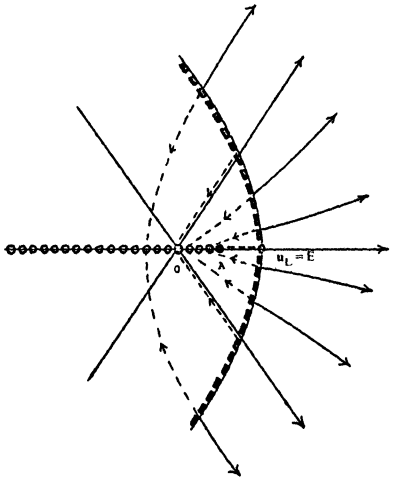

FIG. 4(b). *Solution diagram for* $\theta_L = 0$.

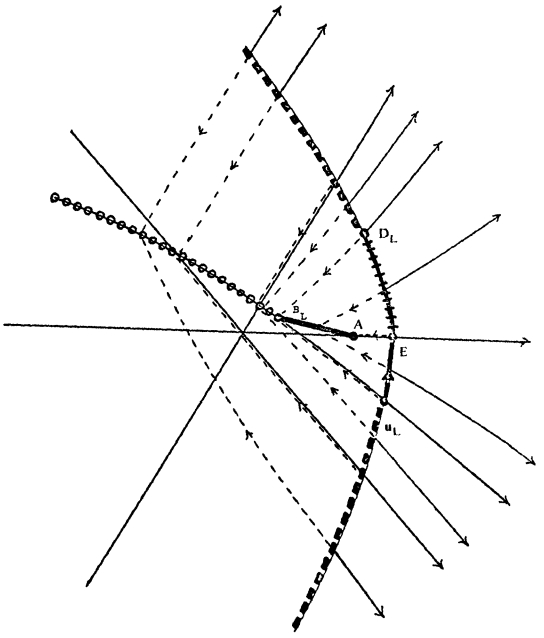

FIG. 4(c). *Solution diagram for* $\mathbf{u}_L \in \mathscr{A}_1$.

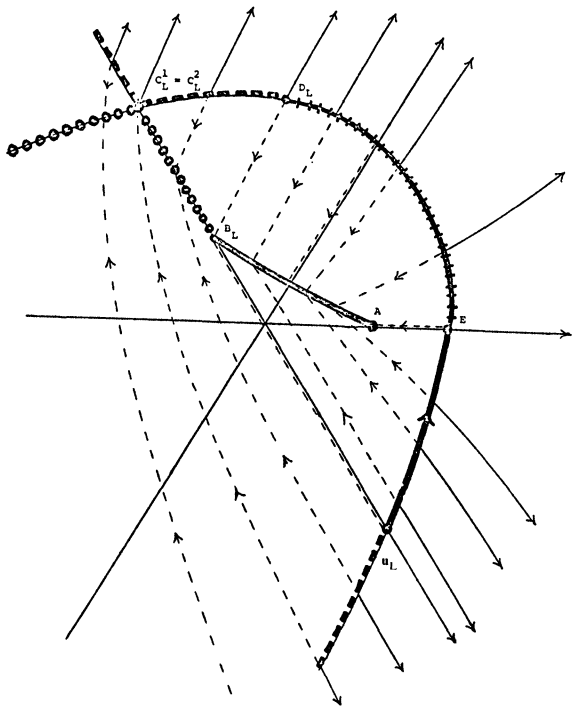

FIG. 4(d). *Solution diagram for* $\theta_L = \theta_{12}$.

3. Solution of the Riemann problem

3.1. In Figs. 4(a)–(j) we give the solution of the Riemann problem for the symmetric systems (1) in Region III. In each diagram, $\mathbf{u}_L$ is fixed and an arbitrary point represents $\mathbf{u}_R$. Figures 4(c), (e), (g) and (i) depict the solutions for $\mathbf{u}_L$ in sectors $\mathscr{A}_1$, $\mathscr{A}_2$, $\mathscr{A}_3$ and $\mathscr{A}_4$, respectively, in each of which the solution diagrams are qualitatively the same. For completeness, we include solution diagrams for $\mathbf{u}_L$ on the boundaries of these sectors: the ray $\theta = \theta_{12}$ is the axis separating sectors $\mathscr{A}_1$ and $\mathscr{A}_2$, and the ray $\theta = \theta_{34}$ is the axis separating sectors $\mathscr{A}_3$ and $\mathscr{A}_4$. The ray $\theta = \theta_*$, which separates sectors $\mathscr{A}_2$ and $\mathscr{A}_3$, is the key ray on which $\lambda_1 = 0$.

In each solution diagram, the 1-wave curve $\mathscr{W}_1(\mathbf{u}_L)$ consists of the union of the 1-shock, 1-rarefaction and 1-composite curves for $\mathbf{u}_L$ (see § 3.2). For each point $\mathbf{u}_M \in \mathscr{W}_1(\mathbf{u}_L)$, the portion of the 2-wave curve $\mathscr{W}_2(\mathbf{u}_M)$ appearing in the diagrams is obtained by proceeding from $\mathbf{u}_M$ along 2-shock and 2-rarefaction curves as far as possible in the direction of the arrows.

The solution of the Riemann problem $\langle \mathbf{u}_L, \mathbf{u}_R \rangle$ consists of a 1-wave with left state $\mathbf{u}_L$ and right state $\mathbf{u}_M$, followed by a 2-wave with left state $\mathbf{u}_M$ and right state $\mathbf{u}_R$ where the intermediate state $\mathbf{u}_M$ is determined as follows: start from $\mathbf{u}_R$ and follow the 2-wave curve backwards from $\mathbf{u}_R$ (opposite the direction of the arrows) until you reach a point $\mathbf{u}_M$ in $\mathscr{W}_1(\mathbf{u}_L)$. The state $\mathbf{u}_M$ so constructed satisfies $\mathbf{u}_R \in \mathscr{W}_2(\mathbf{u}_M)$ and defines the waves in the solution. This procedure is not well-defined precisely when $\mathbf{u}_R$ is in either the compressive portion of $\mathscr{H}(\mathbf{u}_L)$ or the triple shock curve. (The triple shock curve is $[AB_L]$ in Figs. 4(c)–(e) and is $[-\mathbf{u}_*A]$ in Figs. 4(f), (g). There is no triple shock curve in the other figures). In the case of ambiguity, the solutions are unique in the x,t-plane since then all shock speeds that occur are equal. This ensures continuous dependence of the solution on $\mathbf{u}_L$ and $\mathbf{u}_R$.

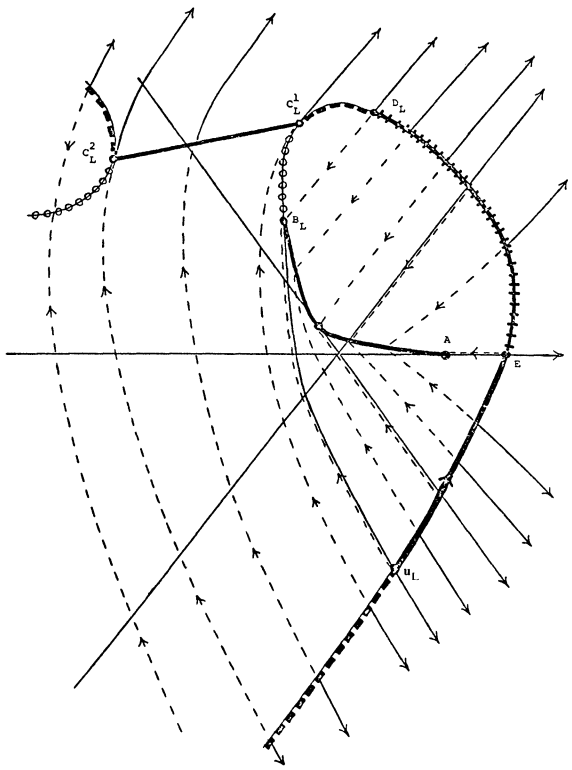

FIG. 4(e). *Solution diagram for* $\mathbf{u}_L \in \mathscr{A}_2$.

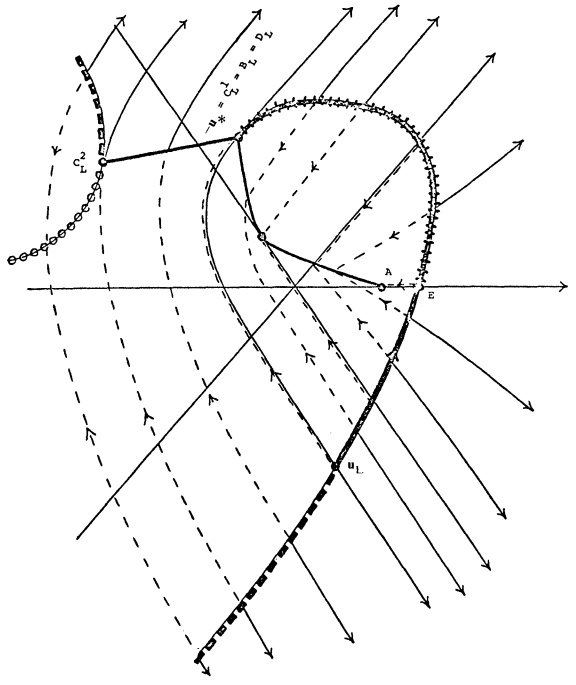

FIG. 4(f). *Solution diagram for* $\theta_L = \theta_*$.

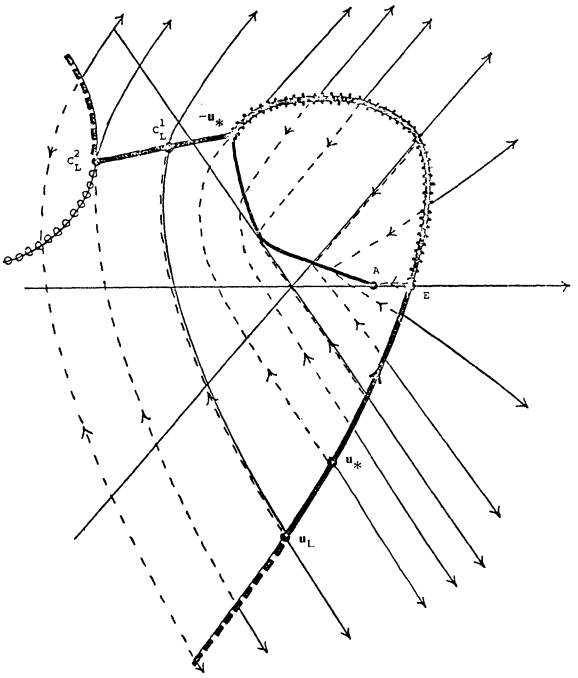

FIG. 4(g). *Solution diagram for* $\mathbf{u}_L \in \mathcal{A}_3$.

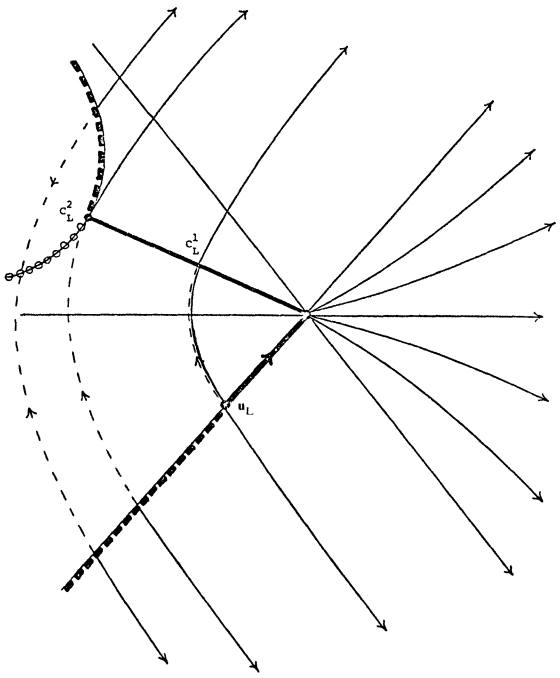

FIG. 4(h). *Solution diagram for* $\theta_L = \theta_{34}$.

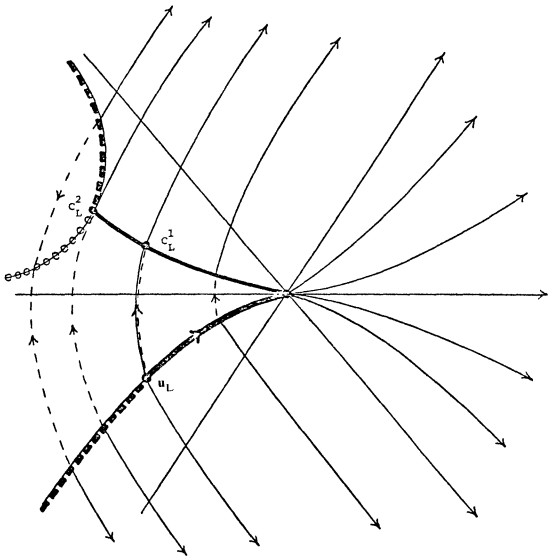

FIG. 4(i). *Solution diagram for* $\mathbf{u}_L \in \mathcal{A}_4$.

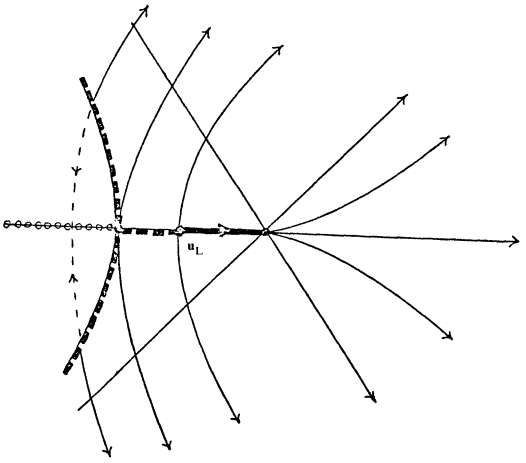

FIG. 4(j). *Solution diagram for* $\theta_L = -\pi$.

3.2. Legend. →→— 1-rarefaction; —— 1-expansive shock; – – – 1-shock; →→— 2-rarefaction; ═══ 2-expansive shock; – –→– – 2-shock (with or without arrows); →→▒▒ 1-composite (rarefaction followed by shock at characteristic speed); —○— compressive shock; —×— crossing shock; —□— expansive shock; ▬▬ 2-boundary, triple shock curves; —— Hugoniot locus of $\mathbf{u}_L$ and u-axis.

Note 1. Arrows on rarefaction curves indicate the direction of increasing eigenvalue. Arrows on shock curves indicate the direction of decreasing shock speed.

Note 2. 1- and 2-shocks in the Hugoniot locus of $\mathbf{u}_L$ are indicated by dashed lines supported by the solid line for the Hugoniot locus.

Acknowledgments. We wish to acknowledge the assistance of Dan Marchesin and Bradley Plohr with the numerical aspects of the problem. We also thank Michael Shearer and David Schaeffer for helpful discussions on many aspects of quadratic Riemann problems. Finally, we would like to thank Dan and Paulo Paes-Leme for their gracious hospitality during our stay in Brazil.

REFERENCES

[1] R. COURANT AND K. O. FRIEDRICHS, *Supersonic Flow and Shock Waves*, John Wiley, New York, 1948.

[2] G. DARBOUX, *Théorie Générale des Surfaces*, Chelsea, New York, 1972.

[3] E. ISAACSON, *Global solution of a Riemann problem for a non-strictly hyperbolic system of conservation laws arising in enhanced oil recovery*, J. Comp. Phys., to appear.

[4] E. ISAACSON AND B. TEMPLE, *Analysis of a singular hyperbolic system of conservation laws*, J. Differential Equations, 65 (1986), pp. 250–268.

[5] E. ISAACSON, D. MARCHESIN, B. PLOHR AND B. TEMPLE, *The Riemann problem near a hyperbolic singularity* I, SIAM J. Appl. Math., 48 (1988), pp. 1009–1032.

[6] E. ISAACSON AND B. TEMPLE, *Examples and classification of non-strictly hyperbolic systems of conservation laws*, Abstracts of AMS, January 1985; Presented in the Special Session on Non-Strictly Hyperbolic Conservation Laws at the Winter Meeting of the Amer. Math. Soc., Anaheim, January 1985.

[7] B. KEYFITZ AND H. KRANZER, *A system of non-strictly hyperbolic conservation laws arising in elasticity theory*, Arch. Rational Mech. Anal., 72 (1980), pp. 219–241.

[8] ———, *The Riemann problem for a class of conservation laws exhibiting a parabolic degeneracy*, J. Differential Equations 47 (1983), pp. 35–65.

[9] P. D. LAX, *Hyperbolic systems of conservation laws*, II, Comm. Pure Appl. Math., 19 (1957), pp. 537–566.

[10] ———, *Shock waves and entropy*, in Contributions to Nonlinear Functional Analysis, E. H. Zarantonello, ed., Academic Press, New York, 1971, pp. 603–634.

[11] T. P. LIU, *The Riemann problem for general* 2×2 *conservation laws*, Trans. Amer. Math. Soc., 199 (1974), pp. 89–112.

[12] D. G. SCHAEFFER AND M. SHEARER, *The classification of* 2×2 *systems of nonstrictly hyperbolic conservation laws, with application to oil recovery*, with Appendix by D. Marchesin, P. J. Paes-Leme, D. G. Schaeffer and M. Shearer, Comm. Pure Appl. Math., 40 (1987), pp. 141–178.

[13] M. SHEARER, D. G. SCHAEFFER, D. MARCHESIN AND P. J. PAES-LEME, *Solution of the Riemann problem for a prototype* 2×2 *system of non-strictly hyperbolic conservation laws*, Arch. Rational Mech. Anal., 97 (1987), pp. 299–320.

[14] J. A. SMOLLER, *Shock Waves and Reaction Diffusion Equations*, Springer-Verlag, New York, Berlin, Heidelberg, 1982.

[15] B. TEMPLE, *Global solution of the Cauchy problem for a class of* 2×2 *non-strictly hyperbolic conservation laws*, Adv. in Appl. Math., 3 (1982), pp. 335–375.

[16] ———, *Systems of conservation laws with coinciding shock and rarefaction curves*, Contemp. Math., 17 (1983), pp. 143–151.